



You have downloaded a document from  
**RE-BUŚ**  
repository of the University of Silesia in Katowice

**Title:** X-ray diffraction studies of NiTi shape memory alloys

**Author:** Zdzisław Lekston, Eugeniusz Łągiewka

**Citation style:** Lekston Zdzisław, Łągiewka Eugeniusz. (2007). X-ray diffraction studies of NiTi shape memory alloys. "Archives of Materials Science and Engineering" (Vol. 28, iss. 11 (2007), s. 665-672).



Uznanie autorstwa - Użycie niekomercyjne - Bez utworów zależnych Polska - Licencja ta zezwala na rozpowszechnianie, przedstawianie i wykonywanie utworu jedynie w celach niekomercyjnych oraz pod warunkiem zachowania go w oryginalnej postaci (nie tworzenia utworów zależnych).



UNIwersYTET ŚLĄSKI  
W KATOWICACH



Biblioteka  
Uniwersytetu Śląskiego



Ministerstwo Nauki  
i Szkolnictwa Wyższego



# X-ray diffraction studies of NiTi shape memory alloys

Z. Lekston \*, E. Łągiewka

Institute of Materials Science, University of Silesia,  
ul. Bankowa 12, 40-007 Katowice, Poland

\* Corresponding author: E-mail address: zlekston@us.edu.pl

Received 10.10.2007; published in revised form 01.11.2007

## ABSTRACT

**Purpose:** The purpose of this paper is to present the results of the investigations of phase transitions of TiNiCo and Ni-rich NiTi shape memory alloys designed for medical applications.

**Design/methodology/approach:** Temperature X-ray diffraction (TXRD), differential scanning calorimetry (DSC), electrical resistivity (ER) and the temperature shape recovery measurements in three-point bending ASTM 2082-01 tests were used.

**Findings:** It has been found in this work that ageing after solution treatment and annealing below the recrystallization temperature after cold working in the alloys studied create separate reversible  $B2 \leftrightarrow R \leftrightarrow B19'$  transformations. During thermomechanical cycles characteristic temperatures of the reversible  $B2 \leftrightarrow R$  phase transition remain stable. It was concluded that ageing after solution treatment or recovery during annealing after cold working causes the precipitation process and the changes of the defect structure of the alloys promote transitions with the R-phase contribution.

**Research limitations/implications:** The results of the courses of transformations and their characteristic temperatures obtained by TXRD, DSC and ER techniques have a good correlation. Future TXRD research with the use of automatic rapid recording of diffraction patterns during cooling and heating are necessary. The course of phase transitions of the studied alloys determine their applications.

**Practical implications:** The obtained results can be applied into the practice of processing and thermomechanical treatments of NiTi alloys designed for the production of shape memory medical implants and devices which act under the influence of the human body heat. Presented are the conditions of thermomechanical treatment to obtain a wide temperature range for the R-phase existence in the investigated alloys.

**Originality/value:** The paper presents new results of optimization of the thermal treatment of NiTi shape memory alloys to obtain the reversible  $B2 \leftrightarrow R$  transformation used to prepare new shape memory implants and medical devices which exhibit shape recovery at a narrow temperature range below the human body temperature. In this paper it was shown that the temperature X-ray diffraction method can be used for the visualization of transformation courses and obtaining characteristic temperatures of transformations.

**Keywords:** X-ray phase analysis; Metallic alloys; Heat treatment; NiTi shape memory alloys

## METHODOLOGY OF RESEARCH, ANALYSIS AND MODELLING

### 1. Introduction

The NiTi shape memory alloys known as “Nitinol” alloys offer very attractive properties for technical and medical

applications [1, 2]. The shape memory effects are associated with reversible thermoelastic martensitic transformation. Binary alloys, containing 49 – 51 at. % Ni after solution treatment exhibit reversible  $B2 \leftrightarrow B19'$  transformations between a high temperature

B2 phase (austenite) and a low temperature B19' phase (martensite). Characteristic transformation temperatures during cooling are noted as  $M_s$  (Martensite start) and  $M_f$  (Martensite finish) and during heating  $A_s$  (Austenite start) and  $A_f$  (Austenite finish) respectively. High temperature phase in NiTi alloys is considered to be of the CsCl (B2) type, and the martensite a monoclinic distortion of the B19 (AuCd) structure [3, 4]. Often in those alloys, below the characteristic  $T_R$  temperature, the intermediate R-phase occurs, which is considered as a rhombohedral distortion of the B2 structure [5]. When  $T_R > M_s$ , a temperature range in which the rhombohedral R-phase is stable may occur. It is very important that the  $B2 \leftrightarrow R$  transition is reversible in a narrow temperature range of about 5°C unlike the  $B2 \leftrightarrow B19'$  transition which has a temperature hysteresis of about 30°C [6, 7]. The  $B2 \rightarrow R$  transition is characterized by a rapid increase in electrical resistance, extra diffraction spots at 1/3 positions of the B2 reciprocal lattice, extra peaks on the DSC curves and splitting in the  $\{110\}$  and  $\{211\}$  X-ray diffraction reflections [5, 8, 9]. One- or two-way shape memory effects are accompanied by reversible thermoelastic transitions and changes of internal stress in the material during cooling and heating [5, 10]. Superelasticity as the characteristic mechanical behaviour takes place when the change of shape is caused by external stress during loading and unloading. On the stress-strain curves the characteristic long plateau during loading and unloading of the samples is visible [11].

The sequences of transitions, its temperature range, the structure and mechanical and shape memory properties of these alloys strongly depend on the chemical composition and other conditions, such as hot or cold processing, thermal treatment, alloying of other metallic elements and thermal or thermomechanical cycles. It is possible to obtain the stable R-phase by increasing the Ni or Ti content, ageing after solution treatment, annealing at temperatures below the recrystallization temperature following cold working, thermal cycling and substitution of other elements [12,13]. Various techniques, differential scanning calorimetry, electrical resistivity, internal friction, corrosion resistance, shape memory effects and changes of the X-ray or neutron diffraction patterns versus temperature may be used to characterize the structure, transition courses and properties of NiTi alloys [14,15].

For medical applications NiTi implants and devices must have shape memory or superelastic effects at temperatures below the human body temperature.

In this article, the temperature X-ray diffraction investigations to characterize phase transformations of TiNiCo and Ni-rich shape memory alloys designed for medical implants are presented. The purpose was to select a suitable thermal treatment to obtain the reversible  $B2 \leftrightarrow R$  transitions and their shape memory effect in a very narrow temperature range.

## 2. Materials and experiments

$Ti_{50}Ni_{48.7}Co_{1.3}$  and  $Ni_{50.5}Ti_{49.5}$  shape memory alloys were obtained by vacuum induction melting. After homogenization treatment at 900°C for 48 hours in a vacuum furnace, hot pack rolling of ingots to rods was carried out to minimize surface oxidation. Flats and wires were obtained by hot and cold rolling

and drawing. Samples with the required dimensions were mechanically cut and polished.

Solution treatment at 700°C and ageing in the temperature range 300°C-600°C and annealing below recrystallization temperatures after cold deformations were used.

Phase analysis and courses of martensite and reverse transformation were investigated at various temperatures by X-ray diffractometry using Philips diffractometer equipped with a temperature attachment. Diffraction patterns in  $CuK_{\alpha}$  radiation were recorded during cooling and heating rates of 1°C/min in the temperature range from +100 to -120°C.

Characteristic transformation temperatures of specimens after various treatments were determined by DSC method using a Perkin-Elmer DSC-7 calorimeter during cooling from ambient temperature to about -120°C and reheating to about +80°C at the rate of 10°C/min.

The electrical resistivity was recorded during cooling and heating by a 2-point probe using a Diesselhorst compensator.

The shape memory effect of wires was recorded by the bending ASTM 2082-01 test on the measurement state equipped with a PT-100 temperature indicator and LVDT linear variable differential transformer.

## 3. Results and discussion

The X-ray diffractograms of a TiNiCo sample recorded at different temperatures in the diffraction angle range from 37 to 47° (2 $\theta$ ) are shown in Fig. 1-4. A very strong peak 110<sub>B2</sub> of the parent phase is visible at 57°C. During cooling the splitting of the 110<sub>B2</sub> peak caused by rhombohedral distortion of the B2 lattice and the diffraction reflections from (110), (002), (11-1), (020) and (111) planes of martensitic phase appear. The intensities of reflections from the martensitic phase increase, whereas the intensity of the splitting peak decreases together with the decrease in temperature. The very visible reflections of the R-phase and martensitic B19' phase are shown in Fig. 2. At 23°C only very strong reflections of a martensite phase are visible, which is shown in Fig. 3.

After heating above the  $A_f$  temperature, when the peaks from the martensite phase disappear, the identification of other phases as  $Ti_2Ni$ ,  $Ni_3Ti$ ,  $Ni_4Ti_3$ ,  $Ti_4Ni_2O$ ,  $TiO_2$  or TiC and TiN existing in the NiTi alloys is much easier. It is shown in Fig. 4, on the example of the phase identification in a TiNiCo sample, in which after heating up to 97°C the  $Ti_2Ni$  phase has been disclosed. It is possible that in this case on the peaks of the  $Ti_2Ni$  phase the peaks of  $Ti_4Ni_2O$  oxide also overlap.

The X-ray diffraction patterns at different temperatures during cooling and heating of TiNiCo and NiTi alloys after various thermal treatments are shown in Fig. 5–8. After solution treatment of the TiNiCo alloy at 700°C for 15 minutes, during cooling from the room temperature, the decrease of the 110 B2 peak intensity and its broadening are visible. At 11°C clear diffraction peaks of the martensite phase can be seen. Their intensity increases with the decrease in temperature. At -60°C the small splitting of the 110<sub>B2</sub> peak accompanied by rhombohedral distortion of the B2 lattice is shown in Fig. 5. During heating the intensity of the martensite peaks decreases and the diffraction peak of the parent phase increases. At 36°C small diffraction peaks of the martensite phase still remain.

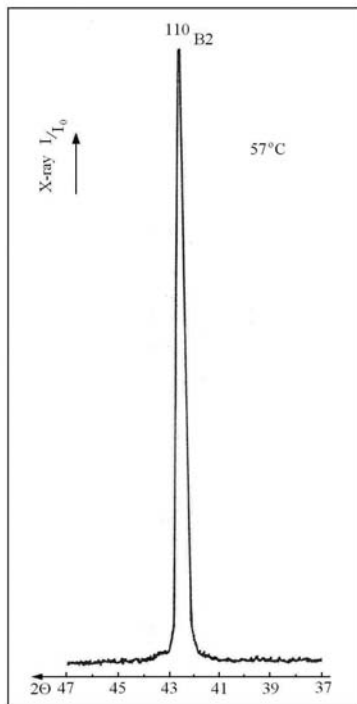


Fig. 1. X-ray diffractogram of TiNiCo alloy recorded in the parent phase state

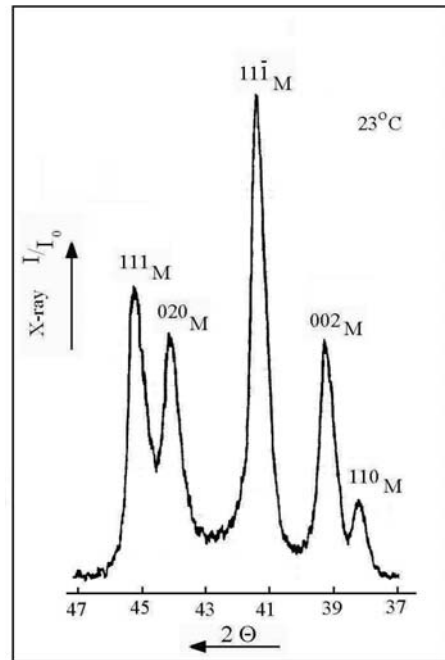


Fig. 3. X-ray diffractogram of TiNiCo alloy recorded in the martensite B19'-phase state

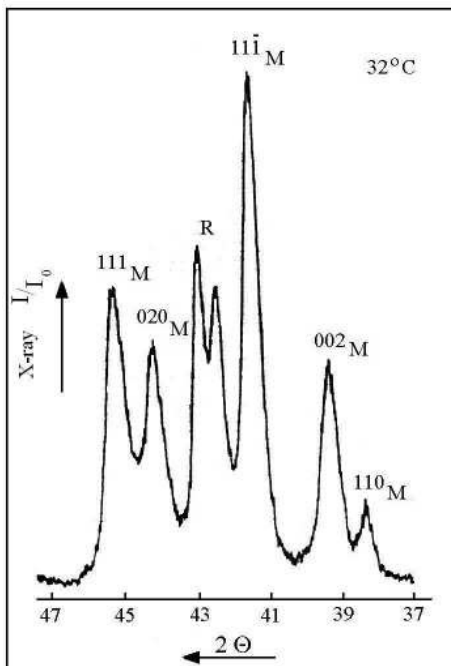


Fig. 2. X-ray diffractograms of TiNiCo alloy in mixture R- and martensite phase state

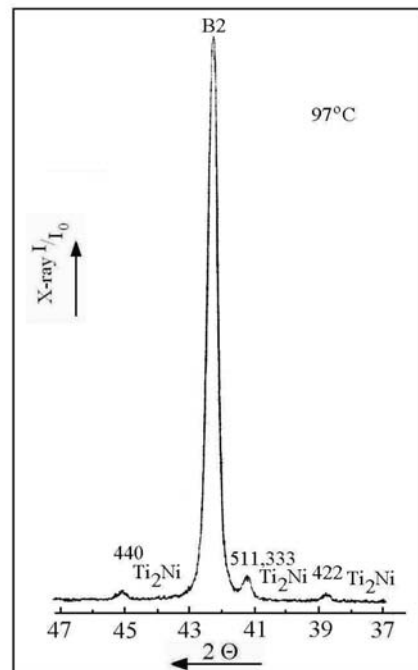


Fig. 4. X-ray diffractogram of TiNiCo alloy recorded after heating above  $A_f$  temperature (the peaks of the  $Ti_2Ni$  intermetallic phase are visible)

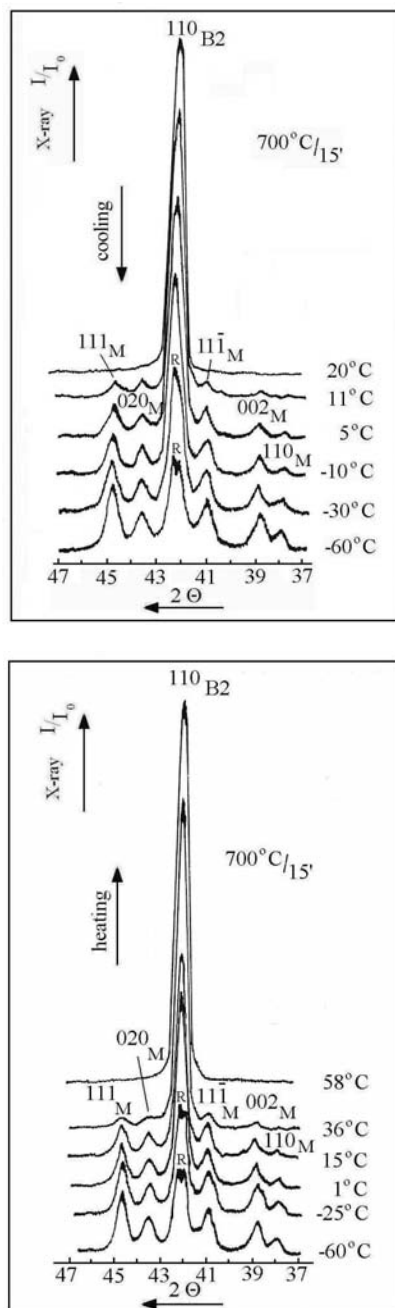


Fig. 5. XRD patterns recorded during cooling and heating of TiNiCo alloy after solution treatment

Resolvable splittings of the  $110_{B2}$  peak were observed during cooling of the samples after ageing at temperatures of 500, 400 and 300°C. The example of diffraction patterns recorded during cooling and heating for the sample after ageing at 300°C is shown in Fig. 6. During cooling the sequences  $B2 \Rightarrow R \Rightarrow B19'$  were registered, whereas during heating the martensite  $B19'$  transforms itself directly into the  $B2$  parent phase.

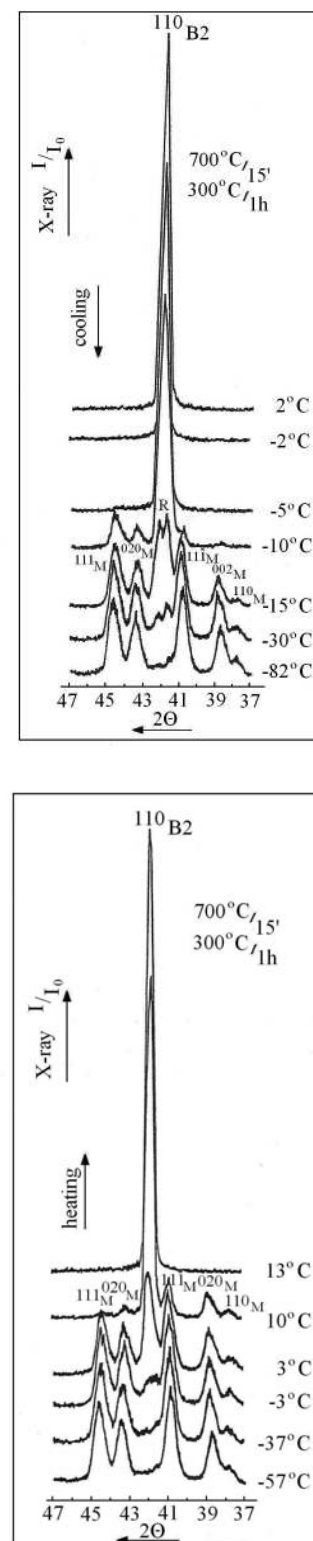


Fig. 6. XRD patterns recorded during cooling and heating of TiNiCo alloy after solution treatment and ageing at 300°C

Identical phase transformation courses were recorded in Ni-rich NiTi alloy with nominal chemical composition Ti-50,5 at.% Ni, in which the reversal phase transitions  $B2 \leftrightarrow B19'$  during cooling and heating were recorded, which is shown in Fig. 7.

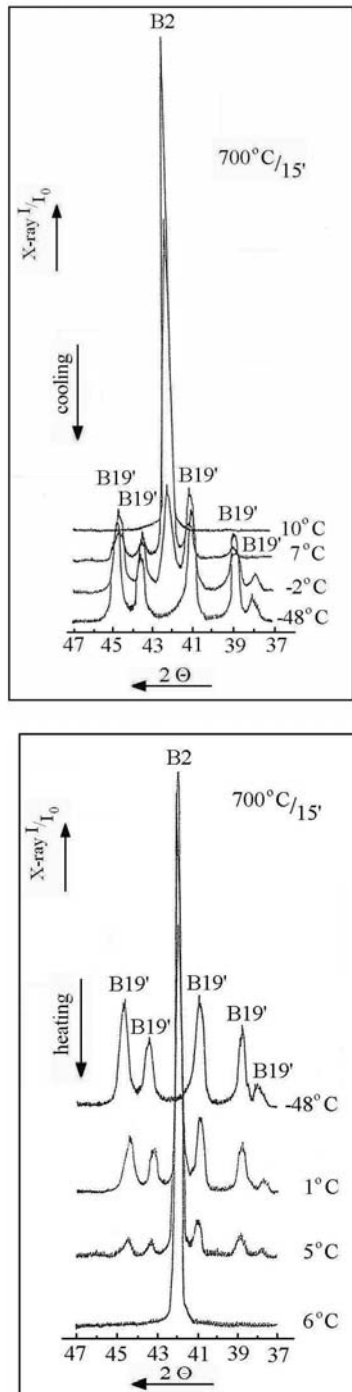


Fig. 7. Transition courses recorded during cooling and heating of Ti – 50,5 at. % Ni alloy after solution treatment

Very good separation of transitions, both during cooling and heating, was obtained after annealing at temperatures below the recrystallization temperature of the alloys after their previous cold working to a deformation of about 40%. The XRD patterns recorded during cooling and heating of TiNiCo alloy after cold rolling and followed by annealing at 450°C for 5 hours with the sequence of transformations  $B2 \leftrightarrow R \leftrightarrow B19'$  are shown in Fig. 8.

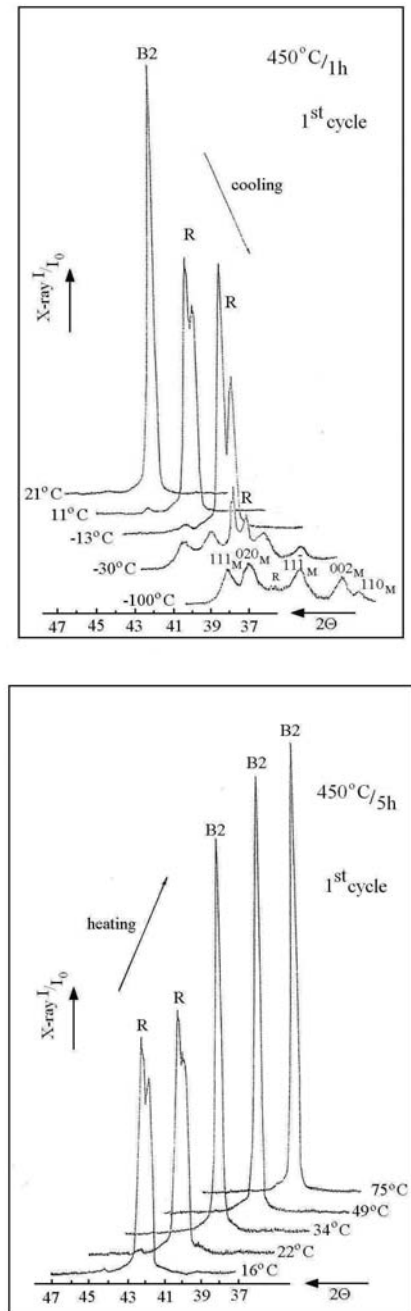


Fig. 8. Changes in the diffraction patterns during cooling and heating of cold worked TiNiCo alloy annealed at 450°C

The separate  $B2 \leftrightarrow R$  and  $R \leftrightarrow B19'$  transitions during cooling and heating after cold processing and annealing of this alloy are also visible on the DSC curves, as is shown in Fig. 9. The samples were cut from wires after cold drawing with the total deformation of 26%. Very good separation, the  $B2 \Rightarrow R$  and  $R \Rightarrow B19'$  transitions are visible on the DSC curves of the samples annealed at 450°C for 30 minutes. The temperatures obtained from exothermal maximum peaks are +20 and -60°C respectively. Similarly, but at a narrower temperature range, the  $B19' \Rightarrow R$  and  $R \Rightarrow B2$  phase transitions are separated during heating. The temperatures obtained from endothermal minimum peaks are +20 and +40°C respectively.

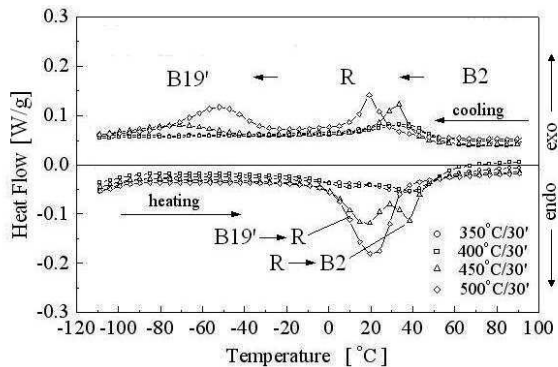


Fig. 9. DSC curves of TiNiCo samples after cold drawing and annealing at different temperatures

The separation of transformations during cooling or heating can be also obtained after ageing or thermomechanical cycling of NiTi alloys. Fig. 10 shows DSC curves of TiNiCo samples after solution treatment at 700°C for 15 minutes and ageing at 500°C for 30 minutes. After solution treatment during cooling there is a two-step transformation  $B2 \leftrightarrow R \leftrightarrow B19'$  and a one-step transformation  $B2 \leftrightarrow B19'$  during heating. Whereas after ageing the transformations are separated during cooling and heating.

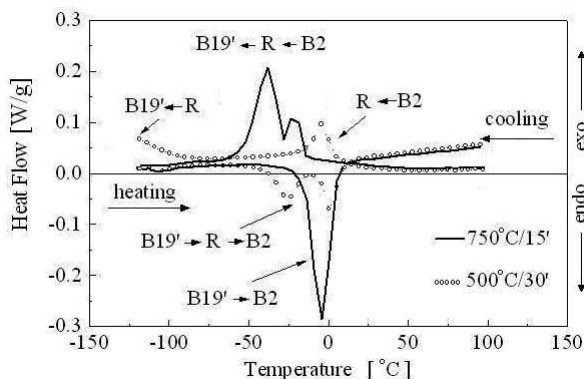


Fig. 10. DSC curves of TiNiCo sample after solution treatment and then ageing at 500°C for 30 minutes

The separation of martensitic transformations in Ni-rich alloys during ageing is explained by preferential formation of  $Ni_4Ti_3$  precipitates along grain boundaries [9]. Probably, the differences in the chemical composition and stresses in the precipitation zone

and in the interior grains, which are precipitate-free, separate the matrix and the transition course is in two-steps  $B2 \Rightarrow R$  and  $R \Rightarrow B19'$ .

Thermally reversible transformations in these alloys were confirmed by electrical resistance changes versus temperature during the cooling-heating cycles. In Fig. 11 and 12 the curves  $\rho(T)$  recorded for TiNiCo and Ni-rich NiTi samples after solution treatment at 700°C for 15 minutes and followed by ageing at 400°C for 1 hour are compared. During cooling the transition of the parent phase B2 to the R-phase occurring below the  $T_R$  temperature is characterized by a rapid increase in electrical resistance. Changes of electrical resistivity can be explained by the changes in electronic density and lattice distortions and changes in the defect structure during transformations [6]. For an alloy with cobalt addition,  $T_R$  is about 25°C, while in the Ni-rich NiTi alloy the R-phase transition begins at -7°C. At the  $M_s$  temperature obtained from the maximum electrical resistance the  $R \Rightarrow B19'$  transition begins. The  $M_s$  temperature in the TiNiCo alloy is +5°C and in the Ni-rich NiTi alloy is -20°C respectively.

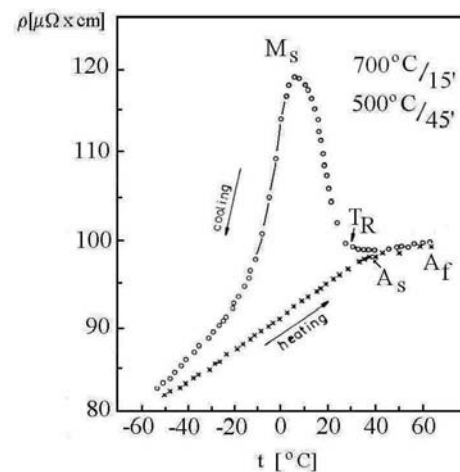


Fig. 11. Electrical resistance as a function of temperature of TiNiCo alloy after solution treatment and ageing

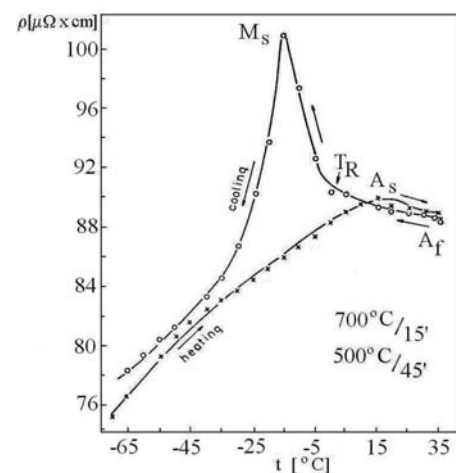


Fig. 12. Electrical resistance as a function of temperature of Ni-rich NiTi alloy after solution treatment and ageing

For practical applications of the shape memory effect associated with the reversal  $B2 \leftrightarrow R$  phase transition, which has a very narrow thermal hysteresis, the knowledge of characteristic temperatures of this transition during cooling and heating is very important. Fig. 13 shows the  $T_R$  (start) temperature of the  $B2 \rightarrow R$  transition during cooling, which is stable in initial thermal cycles and amounts to about  $21^\circ\text{C}$ . In this case the  $T_R$  is chosen when the splitting of the  $110_{B2}$  diffraction peak appears. However, the transformation begins earlier, as the  $110_{B2}$  peak intensity decreases and the full width at half maximum intensity of the  $110_{B2}$  peak is increased.

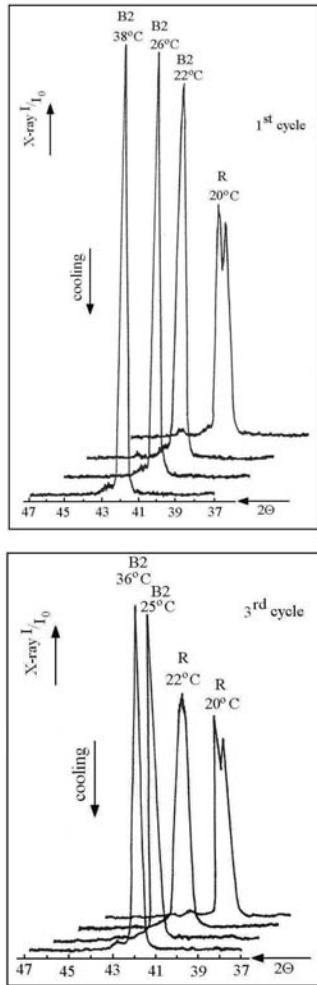


Fig. 13. XRD patterns of TiNiCo alloy at different temperatures, during cooling cycles

Disappearance of splitting was chosen as the  $T_R$  (finish) temperature of  $R \rightarrow B2$  reverse transition during heating. From the X-ray patterns shown in Fig. 14 it appears that this temperature is  $29^\circ\text{C}$  and does not change during thermal cycles. The analysis of the changes of the full width at half maximum intensity of the  $110_{B2}$  peak and the distance between the constituents of the R-doublet or the integrated area under the peak during cooling and heating gives information about the courses and thermal

hysteresis of the  $B2 \leftrightarrow R$  transition. Fig. 15 shows the changes of the full width at half maximum intensity (FWHM) of the  $110_{B2}$  diffraction peak versus temperature, during cooling of the annealed TiNiCo alloy with the sequences of the  $B2 \leftrightarrow R \leftrightarrow B19'$  reversible transformations.

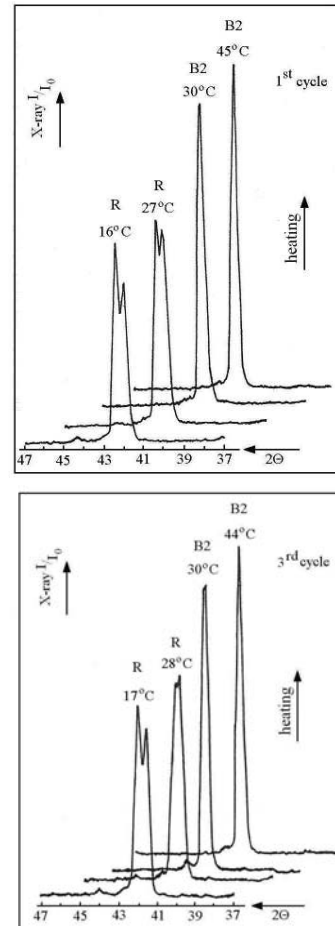


Fig. 14. XRD patterns of TiNiCo alloy at different temperatures during heating cycles

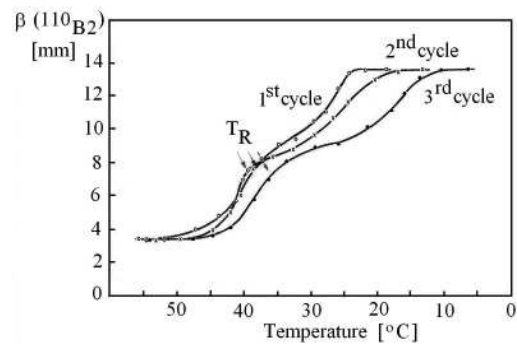


Fig. 15. Changes of FWHM intensity of  $110_{B2}$  diffraction peak with the temperature for heat-treated TiNiCo sample during three succeeding cooling cycles



The shape recovery behaviour during heating in the temperature range of reverse  $R \Rightarrow B2$  transition is shown in Fig. 16. The same specimen was deformed at various temperatures in the temperature range when the material was in the R-phase state. Four thermomechanical cycles were applied. In the first cycle the sample was bent to about  $90^\circ$  in warm water at  $10^\circ\text{C}$  and then shape recovery during heating was recorded. In the next cycles the sample was deformed at 13, 16 and  $19^\circ\text{C}$  respectively. The sample recovered its straight shape at above  $30^\circ\text{C}$ . It is very important for medical applications where the shape memory implant with small temperature hysteresis can be deformed in cool physiological salt.

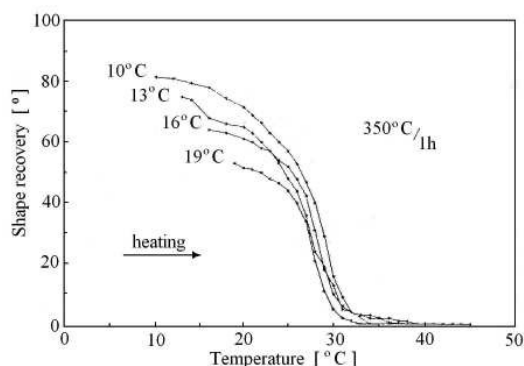


Fig. 16. Shape recovery curves during heating of the TiNiCo sample deformed at various temperatures, below room temperature

#### 4. Conclusions

The studied shape memory alloys exhibit reversible  $B2 \Leftrightarrow R \Leftrightarrow B19'$  transformations. In the alloy with cobalt addition, by annealing at  $450^\circ\text{C}$  for 45 minutes after cold deformation the separation of  $B2 \Leftrightarrow R$  and  $R \Leftrightarrow B19'$  transitions during cooling and heating was achieved. The initial cyclic repetition of  $B2 \Leftrightarrow R$  transition does not change the  $T_R$  and  $A_s$  temperatures. Using the temperature X-ray diffractometry it is possible to observe transformation courses and measure characteristic temperatures of transformations during cooling and heating of the shape memory alloys. The optimization of the thermal treatment and thermomechanical cycling of the studied shape memory alloys to obtain the reversible  $B2 \Leftrightarrow R$  transformation was achieved. It can be used in the projects of new shape memory implants and medical devices with shape recovery at a narrow temperature range below the human body temperature.

#### Additional information

The presentation connected with the subject matter of the paper was presented by the authors during the International

Symposium on Engineering and Education in Bialka Tatrzenska, Poland on 14<sup>th</sup>-16<sup>th</sup> November, 2007.

#### References

- [1] A.R. Pelton, D. Stockel, T.W. Duerig, Medical uses of Nitinol, *Materials Science Forum* 327-328 (2000) 63-70.
- [2] W. Kajzer, M. Kaczmarek, A. Krauze, J. Marciniak, Surface modification and corrosion behavior of Ni-Ti alloy used for urological implants, *Journal of Achievements in Materials and Manufacturing Engineering* 20 (2007) 525-532.
- [3] R.J. Wasilewski, S.R. Butler, J.E. Hanlon, On the Martensitic Transformation in TiNi, *Metals Science Journal* 24 (1967) 104-110.
- [4] K. Otsuka, X Ren, Physical metallurgy of Ti-Ni-based shape memory alloys, *Progress in Materials Science* 50 (2005) 511-678.
- [5] H.C. Ling, R. Kaplow, Phase Transitions and Shape Memory in NiTi, *Metallurgical Transactions* 11A (1980) 77-83.
- [6] T. Goryczka, J. Van Humbeck, Characterization of a NiTiCu shape memory alloy produced by powder technology, *Journal of Achievements in Materials and Manufacturing Engineering* 17 (2006) 65-68.
- [7] J. Uchil, K.P. Mohanchandra, K.K. Mahesh, K. Ganesh Kumara, Thermal and electrical characterization of R-phase dependence on heat-treat temperature in Nitinol, *Physica B253* (1998) 83-89.
- [8] H.C. Ling, R. Kaplow, Variation in the Shape Recovery Temperature in Ni-Ti Alloys, *Materials Science and Engineering* 48 (1981) 241-247.
- [9] J. Khalil Allafi, X. Ren, E. Eggeler, The mechanism of multistage martensitic transformations in aged Ni-rich NiTi shape memory alloys, *Acta Materialia* 50 (2002) 793-803.
- [10] S. Turenne, S. Prokoshkin, V. Brailovski, N. Sacepe, Mechanical and X-ray Characterization of the Assisted Two-Way Shape Memory Effect in NiTi, *Canadian Metallurgical Quarterly* 39 (2000) 217-224.
- [11] Z. Lekston, H. Morawiec, J. Drugacz, Application of superelastic NiTi wires for mandibular distraction, *Materials Science and Engineering A378* (2004) 537-541.
- [12] T. Todoroki, H. Tamura, Effect of Heat Treatment after Cold Working on the Phase Transformation in NiTi Alloy, *Transactions Japan Institute of Metals* 28 (1987) 83-94.
- [13] M. Pattabi, K. Ramakrishna, K.K. Mahehsh, Effect of thermal cycling on the shape memory transformation behavior of NiTi alloy: Powder X-ray diffraction study, *Materials Science and Engineering A* 448 (2007) 33-38.
- [14] J. Uchil, F.M. Braz Fernandes, K.K. Mahesh, X-ray diffraction study of the phase transformations in NiTi shape memory alloy, *Materials Characterization* 58 (2007) 243-248.
- [15] M. Kaczmarek, Corrosion resistance of NiTi alloy in simulated body fluids, *Archives of Materials Science and Engineering* 28/5 (2007) 269-272.